ICARCV '94

THE THIRD INTERNATIONAL CONFERENCE ON AUTOMATION, ROBOTICS AND COMPUTER VISION

9-11 November 1994
Shangri-La, Singapore

PROCEEDINGS

(VOLUME 1 OF 3)

ORGANISED BY

School of Electrical and Electronic Engineering
Nanyang Technological University, Singapore

The Institution of Engineers, Singapore

The Third International Conference on
Automation, Robotics and Computer Vision
(ICARCV '94)
Singapore, November 9-11, 1994

IMPEDANCE CONTROL OF MULTIPLE POINTS OF MANIPULATORS UTILIZING FORCE REDUNDANCY

Toshio TSUJI, Achmad JAZIDIE, Makoto KANEKO and Mitsuo NAGAMACHI

Faculty of Engineering, Hiroshima University
1-4-1, Kagamiyama, Higashi Hiroshima-shi, 724 Japan
E-mail: tsuji@huis.hiroshima-u.ac.jp

Abstract

The present paper proposes an impedance control method using force redundancy based on the *Hierarchical Impedance Control* (HIC) framework and the concept of virtual arms. The proposed method can control not only end-effector impedance but also regulate the impedance of multiple points on the links of the manipulator. The desired end-effector impedance is always realized under the proposed method, since controlling the end-effector impedance is considered as the highest priority task and regulating the multiple points impedance as the sub task.

1. Introduction

Research activities focused on the resolution of redundancy have been increased, including the motion and force redundancy. As regards the force redundancy, Khatib pioneered the use of the null space on the force/torque transformation to control the internal joint motion of redundant manipulators [1]. Kang and Freeman [2] derived the null space damping method for several performance criteria.

On the other hand, impedance control [3], [4] is one of the most effective method that has been suggested for development of the compliant motion. Up to the present, however, a few researches have been reported about using motion redundancy in terms of impedance control such as [5] and [6]. Also, [7] proposed the *Dynamic Direct Compliance Control* using the motion redundancy to obtain an independent joint control torque for realizing the desired end-effector impedance.

Recently, Tsuji and Jazidie [8] have been proposed the *Hierarchical Impedance Control* (HIC) for utilizing force redundancy. It can control not only end-effector impedance using one of the conventional impedance control methods but also additional arm impedance such as joint impedance. The HIC scheme has been introduced by incorporating an additional controller to the end-effector impedance controller in a parallel way. The additional controller is designed in such a way that it has no effect to the dynamic behavior of the end-effector motion.

In the present paper, the HIC framework is applied to develop a method that can control the impedance of multiple points on the links of the manipulator. Previously, [9] and [10] proposed a method called *Multi-Point Compliance Control* (MPCC) which is able to regulate the compliance of several points on the manipulator's links as well as the end-effector compliance. Here, the MPCC is extended to the dynamical case and a new control method called the *Multi-Point Impedance Control* (MPIC) is proposed. Under the proposed method, the desired end-effector impedance can always be realized, since controlling the end-effector impedance is considered as the highest priority task, and the regulating the multiple points impedance as the sub task.

2 Hierarchical impedance control

2.1 HIC scheme

The basic idea and the sufficient condition of the HIC scheme [8] are described in this section. Firstly, the motion equation of an m-joint manipulator can be expressed, in general, as follows.

$$M(\theta)\ddot{\theta} + h(\theta,\dot{\theta}) = \tau + J^T F_e^{ext} , \tag{1}$$

where $F_e^{ext} \in \Re^l$ is the external force exerted on the end-effector; $\theta \in \Re^m$ is the joint angle vector; $M(\theta) \in \Re^{m\times m}$ is the non-singular inertia matrix (hereafter denoted by M); $h(\theta,\dot{\theta}) \in \Re^m$ is the nonlinear term representing the joint torque vector due to the centrifugal, Coriolis, gravity and friction forces; $\tau \in \Re^m$ is the joint control torque vector; $J(\theta) \in \Re^{l\times m}$ is the end-effector Jacobian matrix (hereafter denoted by J); and l is the dimension of the task space.

Now, the target impedance of the end-effector is expressed by

$$M_e d\ddot{X} + B_e d\dot{X} + K_e dX = F_e^{ext} , \tag{2}$$

where $M_e, B_e, K_e \in \Re^{l\times l}$ are the desired inertia, viscosity and stiffness matrices of the end-effector, respectively, and $dX = X - X_d \in \Re^l$ is the deviation vector of the end-effector position from the desired trajectory X_d .

In the HIC scheme, the control law is given by

$$\tau = \tau_{effector} + \tau_{comp} + \tau_{add} , \tag{3}$$

where $\tau_{effector} \in \Re^m$ is the joint torque vector needed to produce the desired end-effector impedance; $\tau_{comp} \in \Re^m$ is the joint torque vector for the nonlinear compensation; and $\tau_{add} \in \Re^m$ is the joint torque vector for the given sub task. For the term $\tau_{effector} \in \Re^m$, the impedance control law without calculation of inverse Jacobian matrix [4] is adopted:

$$\tau_{effector} = J^{\mathrm{T}}[\Lambda\{\ddot{X}_d - M_e^{-1}(B_e d\dot{X} + K_e dX) - \dot{J}\dot{\theta}\} - \{I - \Lambda M_e^{-1}\}F_e^{ext}] \quad , \tag{4}$$

where $\Lambda = (JM^{-1}J^{\mathrm{T}})^{-1} \in \Re^{l \times l}$. Also, the nonlinear compensation in the joint space is used for the simplicity:

$$\tau_{comp} = \tilde{h}(\theta, \dot{\theta}) \ . \tag{5}$$

It is assumed that $\tilde{h}(\theta,\dot{\theta}) = h(\theta,\dot{\theta})$ and manipulator's configuration is not in a singular posture. Moreover, if the additional joint control torque, τ_{add}, satisfies the following condition [8]

$$\bar{J}^{\mathrm{T}}\tau_{add} = 0 \ , \tag{6}$$

where $\bar{J} = M^{-1}J^{\mathrm{T}}\Lambda \in \Re^{m \times l}$, then τ_{add} dynamically has no effect to end-effector motion of the manipulator, and the end-effector impedance remains equal to the target impedance given in (2).

2.2 Optimal additional controller

Kang and Freeman [2] derived three kinds of the general solution of (6) corresponding to the three local joint torque optimization schemes: joint torque minimization, natural joint motion and joint acceleration minimization. Note that the null space derived by joint torque minimization and natural joint motion criteria are the same as the ones used in Tsuji and Jazidie [8] and Khatib [1], respectively.

In the present paper, using the natural joint motion criterion, we will derive the additional optimal controller, τ_{add}, corresponding to the desired joint torque, τ^*_{add}, for a given sub task. Firstly, the null space derived by the natural joint motion criterion is given by

$$\tau_{add} = (I - J^{\mathrm{T}}\bar{J}^{\mathrm{T}})z \ , \tag{7}$$

where $z \in \Re^m$ is an arbitrary vector. The joint torque, τ_{add}, in (7) always satisfies the sufficient condition (6), and now the problem becomes how to find the arbitrary vector z in (7) to minimize the following cost function $G(\tau_{add})$:

$$G(\tau_{add}) = (\tau^*_{add} - \tau_{add})^{\mathrm{T}}M^{-1}(\tau^*_{add} - \tau_{add}) \ . \tag{8}$$

The cost function (8) describes the inertia inverse weighted driving force or the acceleration energy about the discrepency between τ_{add} and τ^*_{add} [2]. By minimizing the cost function (8), the additional joint torque, τ_{add}, would be close to the desired one, τ^*_{add}. Using the least square method, we can find the optimal solution (*see appendix A*) as given by

$$\tau_{add} = (I - J^{\mathrm{T}}\bar{J}^{\mathrm{T}})\tau^*_{add} \ . \tag{9}$$

The joint torque of (9) is the optimal one corresponding to the cost function (8) and has no effect to the dynamic behavior of the end-effector motion, since τ_{add} always lies in the null space of $\bar{J}^{\mathrm{T}}$. So, under the HIC, it is possible to utilize arm redundancy through a suitable selection of the additional controller, τ_{add}, in the sense that the manipulator can perform a sub task while controlling the end-effector impedance.

3 Virtual arm and its kinematics

We consider a redundant manipulator having m joints shown in **Fig.1**. The virtual arm is defined as an arm which has its end-effector (hereafter, referred as a *virtual end-point*) located on a joint or a link of the actual arm [9]. Here, n_v virtual arms are generally considered, corresponding to the number of the virtual end-points which we want to regulate their impedance.

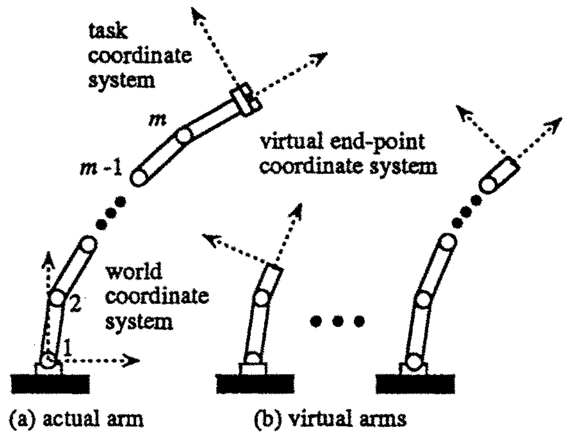

Fig.1 Actual arm and virtual arms

Let the virtual end-point position and velocity vectors of the i-th virtual arm in the i-th virtual end-point coordinate system be denoted as $X_{vi} \in \Re^l$ and $\dot{X}_{vi} \in \Re^l$, respectively. Let also the corresponding force vector be denoted as $F_{vi} \in \Re^l$. For redundant manipulators, m is larger than l. The concatenated instantaneous forward kinematics for all virtual arms is given by

$$\dot{X}_v = J_v\dot{\theta} \ , \tag{10}$$

$$\tau = J_v^{\mathrm{T}}F_v \ , \tag{11}$$

where $\dot{X}_v = [\dot{X}_{v1}^{\mathrm{T}}\ \dot{X}_{v2}^{\mathrm{T}} \cdots \dot{X}_{vn_v}^{\mathrm{T}}]^{\mathrm{T}} \in \Re^{n_v l}$ and $J_v = [J_{v1}^{\mathrm{T}}\ J_{v2}^{\mathrm{T}} \cdots J_{vn_v}^{\mathrm{T}}]^{\mathrm{T}} \in \Re^{n_v l \times m}$ are the concatenated velocity vector and the concatenated Jacobian matrix of the virtual end-points, respectively. $F_v = [F_{v1}^{\mathrm{T}}\ F_{v2}^{\mathrm{T}} \cdots F_{vn_v}^{\mathrm{T}}]^{\mathrm{T}} \in \Re^{n_v l}$ is the concatenated force vector of all virtual end-points. Here, $J_{vi} \in \Re^{l \times m}$ is the Jacobian matrix associated with the i-th virtual arm. In the following section, we will derive the desired additional joint control torque, τ^*_{add}, for controlling the impedance of multiple points on the links of the manipulator using the concept of the virtual arms.

4 Multi-point impedance control

4.1 Multi-point impedance control law

When the manipulator interacts with the environment not only through the actual end-effector but also through other points on the links of the manipulator, the motion equation of the manipulator can be written in the following form:

$$M(\theta)\ddot{\theta} + h(\theta,\dot{\theta}) = \tau + J^{\mathrm{T}}F_e^{ext} + J_v^{\mathrm{T}}F_v^{ext} \quad , \qquad (12)$$

where $F_v^{ext} \in \Re^{n_v l}$ is the concatenated external force vector exerted on the virtual end-points. The joint control torque is given by

$$\tau = \tau_{effector} + \tau_{comp} + \tau_{add} - (\bar{J}J)^{\mathrm{T}}J_v^{\mathrm{T}}F_v^{ext} , \qquad (13)$$

including the cancellation torque, $(\bar{J}J)^{\mathrm{T}}J_v^{\mathrm{T}}F_v^{ext}$, for the effects of the external forces exerted on the virtual end-points to the actual end-effector motion.

Now, the target impedance for the multiple virtual end-points is described as

$$M_v d\ddot{X}_v + B_v d\dot{X}_v + K_v dX_v = F_v^{ext} \; , \qquad (14)$$

where $M_V, B_V, K_V \in \Re^{n_v l \times n_v l}$ are, respectively, the concatenated inertia, viscosity and stiffness of virtual end-points. Here, $dX_{vi} = X_{vi} - X_{vi}^d \in \Re^l$ is the deviation vector associated with the i-th virtual end-point from its desired trajectory, $X_{vi}^d \in \Re^l$.

In order to determine the desired joint torque, τ_{add}^*, for controlling the multiple points impedance, firstly, the effects of τ_{add}^* to the actual end-effector impedance is ignored, i.e., the null space transformation matrix reduces to an identity matrix in (9), then τ_{add} in (13) is equal to τ_{add}^*. Based on the kinematic relationship between the virtual end-point motion and the joint motion (10), we can find the following joint torque for controlling the multiple points impedance:

$$\begin{aligned}\tau_{add}^* = & -J_v^{\mathrm{T}}(M_v d\ddot{X}_v + B_v d\dot{X}_v + K_v dX_v) - \tau_{effector} + \\ & (\bar{J}J)^{\mathrm{T}}J_v^{\mathrm{T}}F_v^{ext} - J^{\mathrm{T}}F_e^{ext} + M(\theta)\ddot{\theta} \; , \end{aligned} \qquad (15)$$

Under the HIC framework, the coupling effects of τ_{add}^* to the actual end-effector impedance can be filtered out through the null space transformation matrix using equation (9), and the additional joint control torque τ_{add} is assured to be always the optimal one corresponding to the cost function (8). Substituting (15) into (9) we have

$$\begin{aligned}\tau_{add} = & -(I - J^{\mathrm{T}}\bar{J}^{\mathrm{T}})\, J_v^{\mathrm{T}}(M_v d\ddot{X}_v + B_v d\dot{X}_v + K_v dX_v) \\ & + (I - J^{\mathrm{T}}\bar{J}^{\mathrm{T}})M(\theta)\ddot{\theta} \end{aligned} \qquad (16)$$

using the following property:

$$(I - J^{\mathrm{T}}\bar{J}^{\mathrm{T}})J^{\mathrm{T}}u = 0 \; , \qquad (17)$$

where $u \in \Re^l$ is an arbitrary vector. The block diagram of the multi-point impedance control proposed in this paper is shown in **Fig.2**.

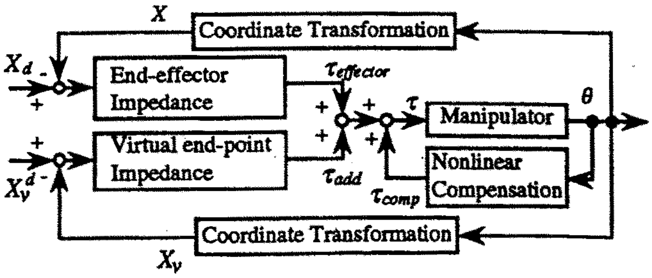

Fig.2 Block diagram of the hierarchical control of multi-point impedance. The method can control the virtual end-points impedance as well as the end-effector impedance of the manipulator.

4.2 Validity of the MPIC

Figure 3 shows four kinematic conditions of a six-joint planar manipulator (m=6; l=2) that can be categorized depending on the number and the location of the virtual end-point as follows [9]: i) the redundant case (Fig. 3(a)), ii) the non-singular case (Fig. 3(b)), iii) the over-constrained case (Fig. 3(c)) and iv) the singular case (Fig. 3(d)). Since the MPIC is developed using the concept of virtual arms, the above four cases are analyzed in this section.

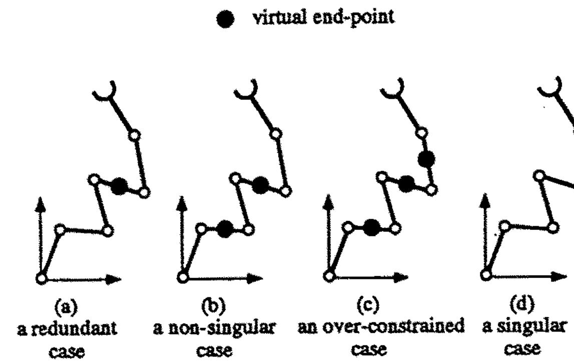

Fig.3 Four cases of the virtual arms

Let define $J_c = [J_v^{\mathrm{T}}\, J^{\mathrm{T}}]^{\mathrm{T}} \in \Re^{(n_v+1)l \times m}$ as the concatenated Jacobian matrix for all virtual arms and the actual arm. The rank of J_c reflects the four cases mentioned above: J_c is of full row rank for the redundant case, of full rank and square matrix for the non-singular case, of full column rank for the over-constrained case, and not of full rank for the singular case.

Now, applying the multi-point impedance control law derived in the previous section (see eqs. (13), (4), (5) and (16)) to the motion equation of the manipulator (12), we can have the following equation:

$$(I - J^{\mathrm{T}}\bar{J}^{\mathrm{T}})J_v^{\mathrm{T}}(M_v d\ddot{X}_v + B_v d\dot{X}_v + K_v dX_v - F_v^{ext}) = 0 \quad . \; (18)$$

It can be seen that the realization of the virtual end-point impedance depends on the rank of the matrix $(I - J^{\mathrm{T}}\bar{J}^{\mathrm{T}})J_v^{\mathrm{T}}$. When $(I - J^{\mathrm{T}}\bar{J}^{\mathrm{T}})J_v^{\mathrm{T}}$ is of full column rank, the target impedance of the virtual end-points (14) can be realized exactly. Otherwise, the impedance of the virtual end-points differs from the desired one. On the other hand, the relationship between the rank of $(I - J^{T}\bar{J}^{T})J_v^{T}$ and the rank of J_c is given by the following theorem.

Theorem 1: When the end-effector Jacobian matrix J is of full row rank matrix, then the matrix $(I - J^{T}\bar{J}^{T})J_v^{T}$ is of full column rank if and only if the concatenated Jacobian matrix J_c is of full row rank.

Proof : See the appendix B. ∎

Hence, it can be seen that in the redundant and non-singular cases (Fig. 3(a) and Fig. 3(b)), the desired multiple points impedance can be realized simultaneously. On the other hand, in the over-constrained and singular cases, the virtual end-point impedance does not agree with the desired one while the end-effector impedance can be controlled exactly.

5 Simulation Experiments

The effectiveness of the proposed method was evaluated by computer simulations using a three-joint planar manipulator (m=3; l=2). The MPIC was applied to the manipulator following a circular trajectory shown in **Fig.4**. The link parameters of the manipulator are shown in **Table 1**.

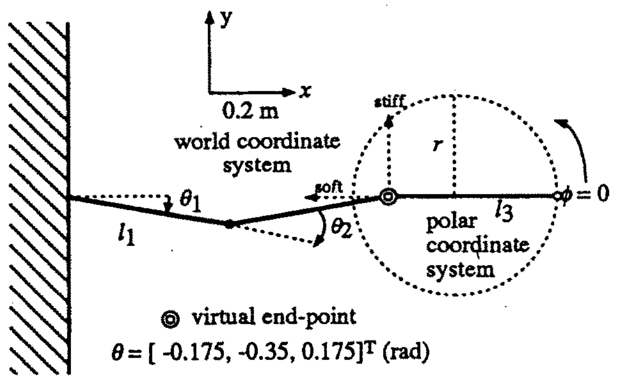

Fig.4 A three-joint planar manipulator following a circular trajectory

TABLE I

LINK PARAMETERS OF THE THREE-JOINT PLANAR MANIPULATOR

	link i $(i = 1, 2, 3)$
length (m)	0.4
mass (kg)	3.0
center of mass (m)	0.2
moment of inertia (kgm^2)	0.32

Two kinds of coordinate systems are chosen as follows: (i) the world coordinate system, X (x, y); and (ii) the polar coordinate system, Φ (ϕ, r), with its origin at the center of the circle where ϕ is the rotational angle and r is the radius of the circular trajectory. The target end-effector impedance (2) is expressed in the polar coordinate system, where the target inertia, viscosity and stiffens matrices are given as M_e = diag. [13.5×10^{-3} (kgm^2), 0.2 (kg)], B_e = diag. [1.25 (Nm/(rad/s)), 2 (N/(m/s))], and K_e = diag. [32.25 (Nm/rad), 5 (N/m)], respectively. Also the desired end-effector trajectory (equilibrium trajectory) is given as the following:

$$\begin{bmatrix} \phi_d(t) \\ r_d(t) \end{bmatrix} = \begin{bmatrix} 20\pi t^3 / t_f^3 - 30\pi t^4 / t_f^4 + 12\pi t^5 / t_f^5 \\ r \end{bmatrix}, \quad (19)$$

where r and the time duration t_f are set to 0.25 m and 2.0 s, respectively. The desired velocity and acceleration of the end-effector are also obtained from (19) by differentiation.

Figure 5 and **Fig.6** show simulation results performed under the conventional impedance control and the MPIC, respectively. The virtual end-point was located on the 3rd joint (n_v = 1: see Fig.4), and the desired virtual end-point impedance matrices are given as M_v = diag. [0, 0.2] (kg), B_v = diag. [0, 20] (N/(m/s)), K_v = diag. [0, 500] (N/m), respect to the world coordinate system. The desired virtual end-point trajectory is given as $X_v^d(t) = X_v(0)$.

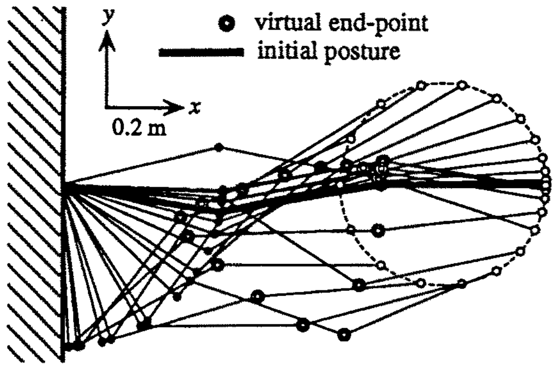

Fig.5 Stick pictures of the three-joint manipulator following a circular trajectory under the conventional impedance control

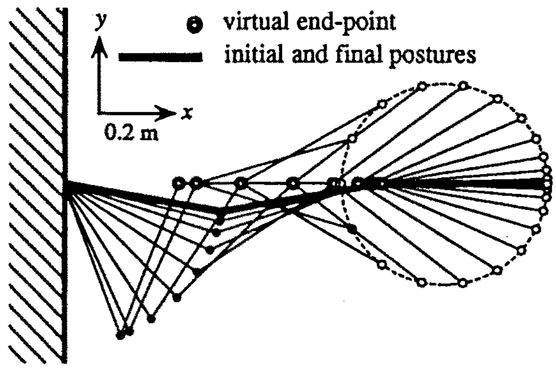

Fig.6 Stick Pictures of the three-joint manipulator following a circular trajectory under the multi-point impedance control. The virtual end-point was located on the 3rd joint of the manipulator.

Under those impedance parameters and the desired trajectory, the virtual end-point moves almost freely in the direction of x axis and constrained tightly in the direction of y axis. From these figures, it can be seen that both of the manipultors can follow the circular trajectory finely. In term of the virtual end-point, however, the effectiveness of the MPIC appear clearly. As expected, in Fig.6 the virtual end-point moves along the x axis during the end-effector follows the circular trajectory.

6 Conclusion

We have proposed the multi-point impedance control for redundant manipulators based on the HIC framework. In this method, controlling the end-effector impedance was considered as the highest priority task and regulating the multiple points impedance as the sub task. Under the proposed method, the desired end-effector impedance can always be realized. It was shown that the method was able to regulate the impedance of several points on manipulator's links without any effect to the end-effector motion. The validity of the MPIC was analyzed and shown by computer simulations.

References

[1] O. Khatib, "Motion/force redundancy of manipulators," *Proc. of Japan-U.S.A. Symposium on Flexible Automation*, 1, pp. 337-342, 1990.

[2] H. J. Kang and R. A. Freeman, "Joint torque optimization of redundant manipulators via the null space damping method," *Proc. IEEE, Int. Conf. on Robotics and Automation*, pp. 520-525, 1992.

[3] N. Hogan, "Impedance control: an approach to manipulation, parts I,II,III," *ASME Journal of Dynamic Systems Control*, vol. 107,no. 1, pp.1-24, 1985.

[4] N. Hogan, "Stable execution of contact tasks using impedance control," *Proc. IEEE International Conference on Robotics and Automation*, pp.1047-1054, 1987.

[5] W. S. Newman and M. E. Dohring, "Augmented impedance control: an Approach to compliant control of kinematically redundant manipulators," *Proc. IEEE International Conference on Robotics and Automation*, pp.30-35, 1991.

[6] Z. X. Peng and N. Adachi, "Compliant motion control of kinematically redundant manipulators," *Trans. on Robotics and Automation*, vol. 9, no. 6, pp. 831-837, 1993.

[7] K. Tanie, K. Yokoi and M. Kaneko, "Compliance control with consideration of trajectory control characteristics," *Proc. of the ASME Int. Computers in Engineering Conf. Exp.*, pp. 275-280, 1990.

[8] T. Tsuji and A. Jazidie, "Impedance control for redundant manipulators: an approach to joint impedance regulation utilizing kinematic redundancy," *J. of the Robotics Society of Japan*, 12-4, pp. 609-615, 1994.

[9] T. Tsuji, T. Takahashi and K. Ito, "Multi-point compliance control for redundant manipulators," In S. Stifter and J.Lenaric Eds.), *Advances in Robot Kinematics*, pp. 427-434, 1991.

[10] A. Jazidie, T. Tsuji, M. Nagamachi and K. Ito, "Multi-point compliance control for dual-arm robots utilizing kinematic redundancy," *Trans. of the SICE*, vol. 29, no. 6, pp.637-646, 1993.

[11] V. Potkonjak and M. Vukobratovic, "Two new methods for computer forming of dynamic equation of active mechanisms", *Mechanism and Machine Theory*, vol. 14, no. 3, pp. 189-200, 1987.

[12] D. L. Bentley and K. L. Cooke, *Linear Algebra with Differential Equations*. Holt, Reinhart and Winston, Inc., pp. 154-155, 1973.

Appendix A

Substituting (7) into (8), we find

$$G(z)=\{\tau^*_{add}-(I-J^{\mathrm{T}}\bar{J}^{\mathrm{T}})z\}^{\mathrm{T}}M^{-1}\{\tau^*_{add}-(I-J^{\mathrm{T}}\bar{J}^{\mathrm{T}})z\}. \quad (A.1)$$

It is well known that the necessary condition regarding the optimal solution of the above problem is given by

$$\partial G(z)/\partial z=0 . \quad (A.2)$$

Substituting (A.1) into (A.2) and expanding it using the properties: $(I-J^{\mathrm{T}}\bar{J}^{\mathrm{T}})^{\mathrm{T}}M^{-1}=M^{-1}(I-J^{\mathrm{T}}\bar{J}^{\mathrm{T}})$ and $\bar{J}JM^{-1}=\bar{J}JM^{-1}J^{\mathrm{T}}\bar{J}^{\mathrm{T}}=M^{-1}J^{\mathrm{T}}\bar{J}^{\mathrm{T}}$ finally we have

$$(I-J^{\mathrm{T}}\bar{J}^{\mathrm{T}})z=(I-J^{\mathrm{T}}\bar{J}^{\mathrm{T}})\tau^*_{add} . \quad (A.3)$$

Then substituting (A.3) into (7), we can obtain

$$\tau_{add}=(I-J^{\mathrm{T}}\bar{J}^{\mathrm{T}})\tau^*_{add} . \quad (A.4)$$

Appendix B

Proof of Theorem 1: For the composite transformation $(I-J^{\mathrm{T}}\bar{J}^{\mathrm{T}})J_v^{\mathrm{T}}$, we have [12]

$$\mathrm{r}((I-J^{\mathrm{T}}\bar{J}^{\mathrm{T}})J_v^{\mathrm{T}})+\dim(R(J_v^{\mathrm{T}})\cap N(I-J^{\mathrm{T}}\bar{J}^{\mathrm{T}}))=\mathrm{r}(J_v^{\mathrm{T}}) , \quad (B.1)$$

where $r(\cdot)$ and $\dim(\cdot)$ denote the rank of the matrix and the dimension of the space, respectively. Also, $R(\cdot)$ and $N(\cdot)$ stand for the range space and the null space of the matrix, respectively.

Firstly, let's assume that the matrix $(I-J^{\mathrm{T}}\bar{J}^{\mathrm{T}})J_v^{\mathrm{T}}$ is of full column rank. This means that J_v is the full row rank matrix, since the matrix $(I-J^{\mathrm{T}}\bar{J}^{\mathrm{T}})$ is not of full rank:

$$\mathrm{r}((I-J^{\mathrm{T}}\bar{J}^{\mathrm{T}})J_v^{\mathrm{T}})=\mathrm{r}(J_v^{\mathrm{T}}) . \quad (B.2)$$

Using (B.1) and (B.2) we obtain

$$R(J_v^{\mathrm{T}})\cap N(I-J^{\mathrm{T}}\bar{J}^{\mathrm{T}})=\{0\} . \quad (B.3)$$

On the other hand, it can be shown that

$$N(I-J^{\mathrm{T}}\bar{J}^{\mathrm{T}})=R(J^{\mathrm{T}}) . \quad (B.4)$$

Substituting (B.4) into (B.3) we can find

$$R(J^{\mathrm{T}})\cap R(J_v^{\mathrm{T}})=\{0\} , \quad (B.5)$$

which implies that J_c is the full row rank matrix.

Now, let's assume that J_c and J_v are the full row rank matrices. Then, $R(J^{\mathrm{T}})\cap R(J_v^{\mathrm{T}})=\{0\}$. As $N(I-J^{\mathrm{T}}\bar{J}^{\mathrm{T}})=R(J^{\mathrm{T}})$, this implies that $(I-J^{\mathrm{T}}\bar{J}^{\mathrm{T}})J_v^{\mathrm{T}}$ is of full column rank. This completes the proof. ■